BALKANTRIB'O5
5th INTERNATIONAL CONFERENCE ON TRIBOLOGY
JUNE.15-18. 2005
Kragujevac, Serbia and Montenegro

WEAR DEVELOPMENT ON CEMENTED CARBIDE INSERTS, COATED WITH VARIABLE FILM THICKNESS IN THE CUTTING WEDGE REGION

K.-D. Bouzakis[1], S. Hadjiyiannis[1], G. Skordaris[1], I. Mirisidis[1], N. Michailidis[1], K.Efstathiou[1]
G. Erkens[2]
[1]Laboratory for Machine Tools and Manufacturing Engineering, Mechanical Engineering Department, Aristoteles University of Thessaloniki, GR-54124, Greece
[2]CemeCon AG, Adenauerstr, 20B1, D-52146 Würselen, Germany

Abstract

During the Physical Vapour Deposition of coatings, the orientation of cemented carbides insert surfaces to the plasma flux direction affects the film thickness distribution on the rake and flank, which in turn might influence the wear propagation in cutting processes. The cutting performance in milling of PVD TiAlN coated cemented carbide inserts with various thicknesses on the rake and flank is introduced and with the aid of FEM-supported calculations explained. The investigation results revealed that a thicker film on the tool rake in comparison to the one on the flank and moreover a thick and uniformly deposited film in the cutting wedge region significantly enhances the cutting performance in milling.

Keywords: *PVD coatings, thickness distribution, cutting performance*

1. INTRODUCTION

The evolution of Physical Vapour Deposition (PVD) technologies facilitated the development of enhanced cutting tool coating materials and thus contributed to an improvement in the manufacturing processes productivity [1,2]. On the other hand a series of parameters such as the substrate pre-treatment [3,4], the cutting edge geometry [5], the film properties [6,7] etc. influence the effectiveness of coated tools in cutting applications. Furthermore the coating thickness distribution on the tool rake and flank, depending on the tool fixturing geometry and kinematics in the vacuum chamber during the film deposition, might significantly affect the cutting tool performance.

The plasma flux during the PVD procedure in the vacuum chamber is guided from the targets to the fixtures, in which the specimens to be coated are placed. In the left part of figure 1, a characteristic arrangement of the targets and a specimen fixture is shown. In general, in order to achieve a uniformly distributed coating on all insert surfaces, three kinds of rotational motions are applied, the rotation of the basic plate ω_P, of each satellite station ω_S and of each specimen fixture ω_f. Moreover the orientation of a cutting insert in relation to the plasma fluxes plays an important role in the distribution of the coating thickness in the cutting wedge region. In the bottom part of the figure, two potential insert positions against the plasma flux are illustrated. If the plasma flux is quasi parallel to the insert rake, a formation of a thicker coating on the flank in comparison to the corresponding one on the rake is expected. Keeping the magnetic field constant and placing the specimen rake vertically to the plasma flux, a coating with reverse thickness characteristics on the tool rake and flank in relation to the previous case can be obtained.

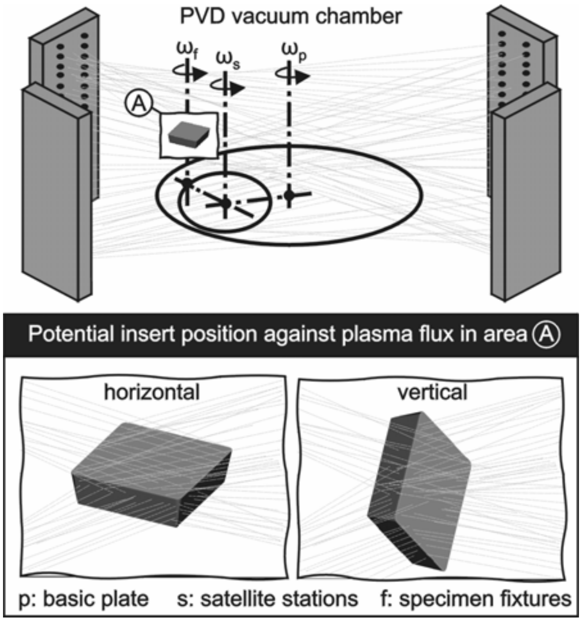

Figure 1: *Potential cutting insert positions and fixtures kinematics during physical vapour deposition (PVD) of coatings.*

In this way cutting inserts can be coated with variable film thickness on the rake and flank depending on the incidence directions of the plasma flux to the insert rake. The cutting performance of such inserts was examined in milling.

2. COATING THICKNESS DISTRIBUTIONS AND MECHANICAL PROPERTIES OF THE APPLIED CUTTING INSERTS

In the frame of this investigation a portion of approximately 40 cemented carbide inserts with the same technical specifications, as shown in the bottom part of figure 2, were coated with $(Ti_{35}Al_{65})N$ films via a High Ionization Sputtering (HIS) PVD process. During the PVD-process the orientation of the specimens against the plasma fluxes was set according to the desired film thickness on the tool rake and flank. The positioning of the specimens was realized through appropriate insert fixtures. The coating thicknesses of all coated cemented carbide inserts on the flank and on the rake near the cutting edge were measured by means of ball cratering tests and classified into three groups, as shown in figure 2. The first group is characterized as "symmetric", consisting of specimens with almost equal coating thickness on rake and flank. In the "symmetric" inserts case, the maximum coating thickness on the rake was approximately 4.2 µm and the corresponding one on flank 3.3 µm.

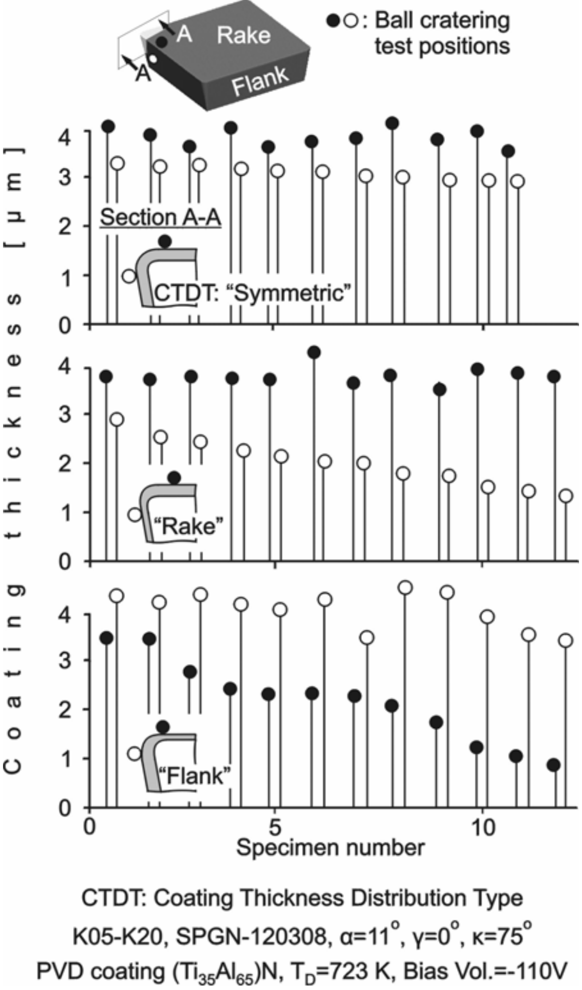

Figure 2: *Classification of the applied cemented carbide inserts according to the coating thickness on their tool rake and flank.*

Second group is "rake" type, having an increased coating thickness on the rake (ca. 4 µm) in comparison to the flank, as illustrated in the middle diagram. The film thickness on flank was in the range from 1.2 µm to 2.9 µm. The third group is "flank" type. In this group the coating thickness on the flank (between 3.5 and 4.5 µm) was always thicker than the corresponding variable one on the rake, the range of which was between 3.5 and 1 µm.

Figure 3 illustrates characteristic columnar as well as amorphous microstructures of PVD coatings versus their thickness. The coating growth mechanisms lead to increased superficial grains size, whereas on an intermediate plane, parallel to the substrate surface, the corresponding grains size is smaller [8,9,10]. The superficial grains size growth of thicker films affect the surface roughness, as illustrated coarser microstructure, a diminishing of the mechanical strength properties of coating materials versus their thickness is expected [6,7].

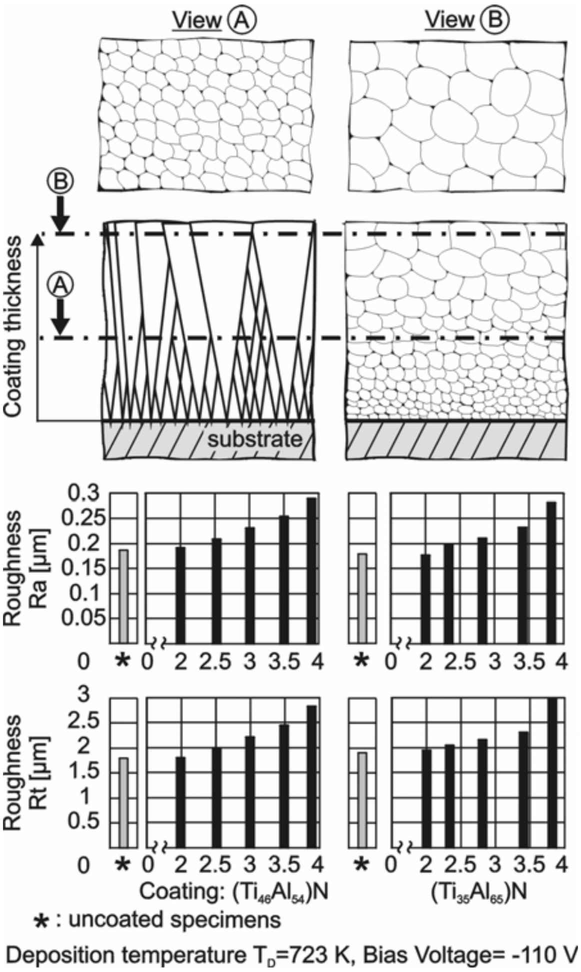

Figure 3: Microstructures of TiAlN coatings and superficial roughnesses.

The stress–strain curves of the examined coatings were determined by means of nanoindentations and a FEM supported evaluation method, as described in the literature [11,12]. The results showed that, as it was expected, the maximum nanoindentation depth h_{max} increases with the coating thickness (see figure 4a). Thus the coating thickness either on the flank or on the rake affects the mechanical strength properties, as already reported in the literatures [6,7]. The probability distributions of the maximum indentation depth [6], demonstrated separately for thin and thick coatings, are shown in figure 4b. The decreasing of the nominal indentation depth (NID) in the thinner coatings compared to the thicker ones is in the bottom figure part. In this way, due to the evident. Considering the nanoindentation results corresponding to the nominal indentation depths of the described thin and thick coatings, the associated stress strain curves were determined [11].

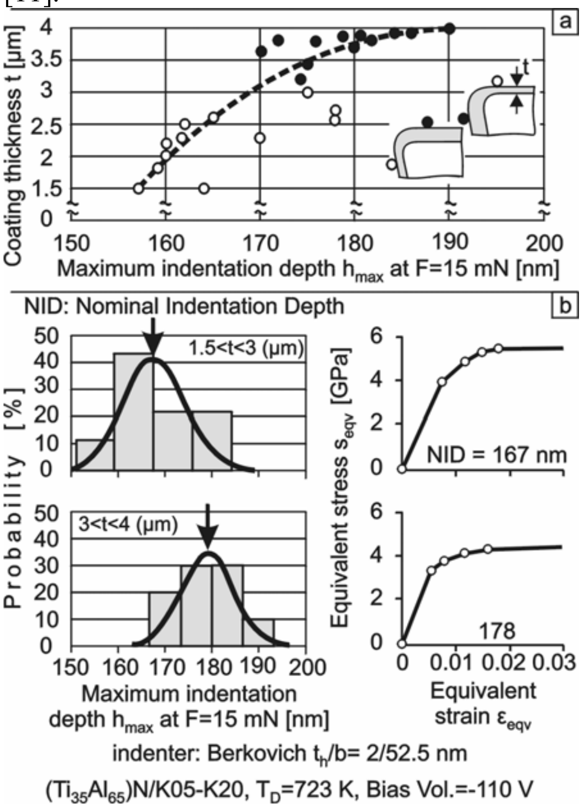

Figure 4: Coating strength properties detected through evaluation of nanoindentation results.

As shown in the right part of figure 4b, an increase in the coating thickness deteriorated the coating mechanical strength properties, whereas the elasticity modulus remained constant.

3. THE EFFECT OF FILM THICKNESS ON TOOL RAKE AND FLANK ON THE WEAR BEHAVIOUR OF COATED INSERTS IN MILLING

In order to investigate the effect of the coating thickness distribution in cutting wedge regions on cutting performance, milling tests were carried out. The tool-workpiece arrangement is illustrated in figure 5a. The experiments were performed using a 3-axis numerically controlled milling centre. A prescribed number of successive cuts was set before every inspection of the cutting insert wear status. The tool wear condition was examined by means of Scanning Electron Microscopy (SEM) and Energy Dispersive Xray (EDX) microanalyses. Figure 5b and c demonstrate flank wear developments versus the accumulated number of cuts of examined coatings, with various film thicknesses on rake and flank.

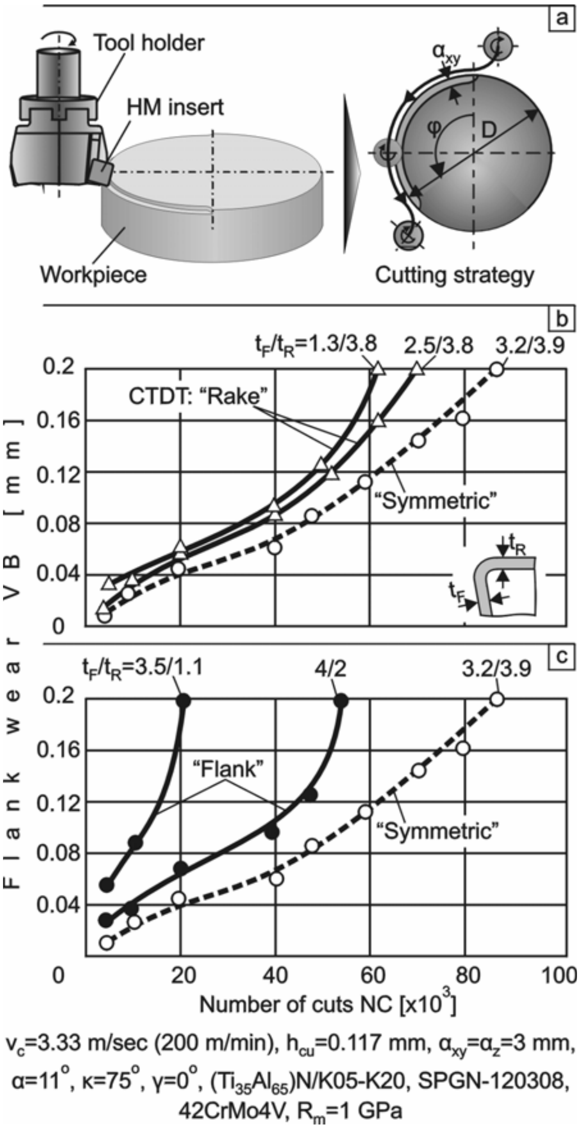

Figure 5: *Milling process kinematics and flank wear development on coated tools with various film thickness on rake and flank.*

The "symmetric" insert type exhibited a better cutting performance in comparison to the "rake" type ones managing to cut approximately 86.000 cuts up to a flank wear of 0.2 mm, whereas in the case of a 1.3 μm coating thickness on the flank only about 60.000 cuts were conducted up to the same flank wear, as shown in figure 5b. On the other hand, a more intensive deterioration of the cutting performance occurs when the coating thickness on the flank of the "flank" type inserts decreases, as shown in figure 5c. In this case, the number of the successive cuts, until a flank wear of 0.2 mm, reduced to only 20.000 cuts at a coating thickness on the rake of 1.1 μm. Hence the milling performance is more affected by the coating thicknesses decreasing on the rake than on the flank. Moreover in all investigated cases the " symmetric" inserts with an almost uniformly distributed thick coating of about 4 μm exhibited the best wear behaviour.

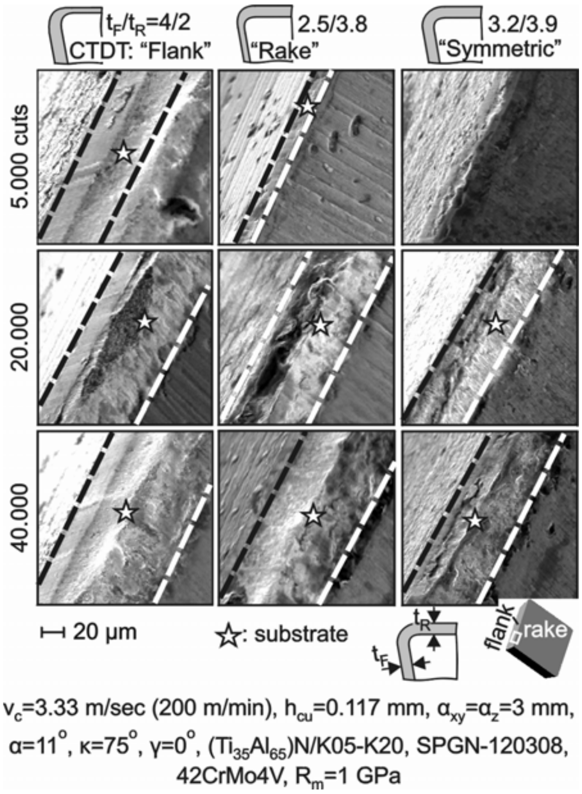

Figure 6: *Wear development on cutting inserts with various coating thickness on the rake and flank.*

The tool wedge wear condition was systematically monitored by means of SEM observations, and EDX microanalyses. The tool wedges after 5.000, 20.000 and 40.000 cuts are illustrated in figure 6. As it can be observed in the upper left SEM micrograph in the case of a "flank" type insert (t_F/t_R [μm]= 4/2), the $(Ti_{35}Al_{65})N$ film was removed very soon, after about 5.000 cuts, from the cutting edge region in both rake and flank. Moreover the bottom left SEM micrograph demonstrates that the flank wear was increased in comparison to all the rest insert cases after the same number of cuts. On the other hand the "symmetric" insert type exhibited an improved milling performance, whereas the coating after 5.000 cuts was undamaged and the wear after 40.000 cuts still limited in the transient region area between the tool rake and flank.

4. FEM SIMULATION OF MILLING CONSIDERING FILM THICKNESS AND STRENGTH PROPERTIES

The FEM simulation of the coated cutting edge and its loads during the material removal process is illustrated in figure 7. The tool wedges are described by plane strain models [13].

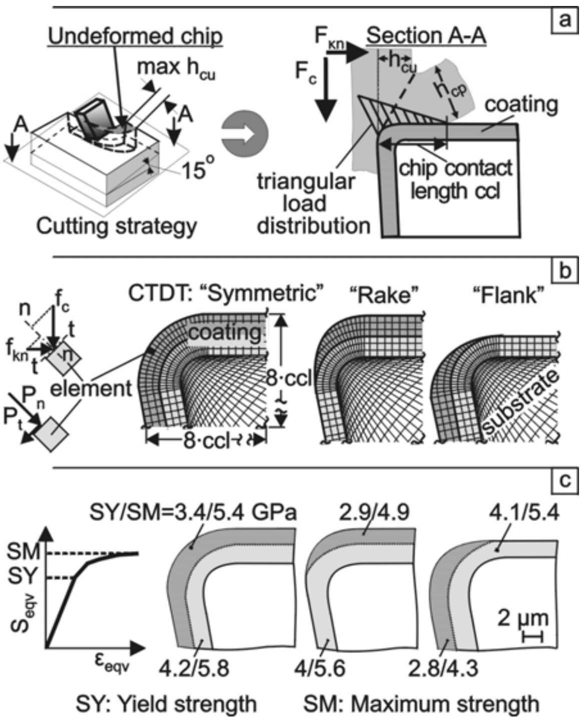

Figure 7*: FEM simulation of the coated cutting edge and of its loads taking into account the film thickness distribution and strength properties.*

The occurring cutting loads, quasi triangularly distributed on the tool rake, are transformed in individual superficial normal (P_n) and tangential (P_t) pressures, acting on each element within approximately the chip contact length ccl (see figure 7a). The cutting force components and the chip contact length were experimentally determined, as it will be described. The FEM simulation considers the film thickness distribution around the cutting wedge and the associated strength properties, as shown in figure 7b and c respectively [6,7].

The cutting force components and the chip contact length ccl were experimentally detected in various coating thickness cases, as it is illustrated in figure 8a. The cutting force components and thus the cutting energy remained practically constant in all coating thickness distributions on the rake and flank, whereas all corresponding force deviations from the "symmetric" coating thickness distribution insert type were lower than 2 %. On the other hand the chip contact length varies according to the film thickness distribution over the cutting wedge, as it is presented in figure 8b. The chip contact length, was measured by means of micrographs as that one shown in the middle figure part, whereas the contact between the chip and the coating surface is brighter, due to the friction of the flowing chip over the tool rake.

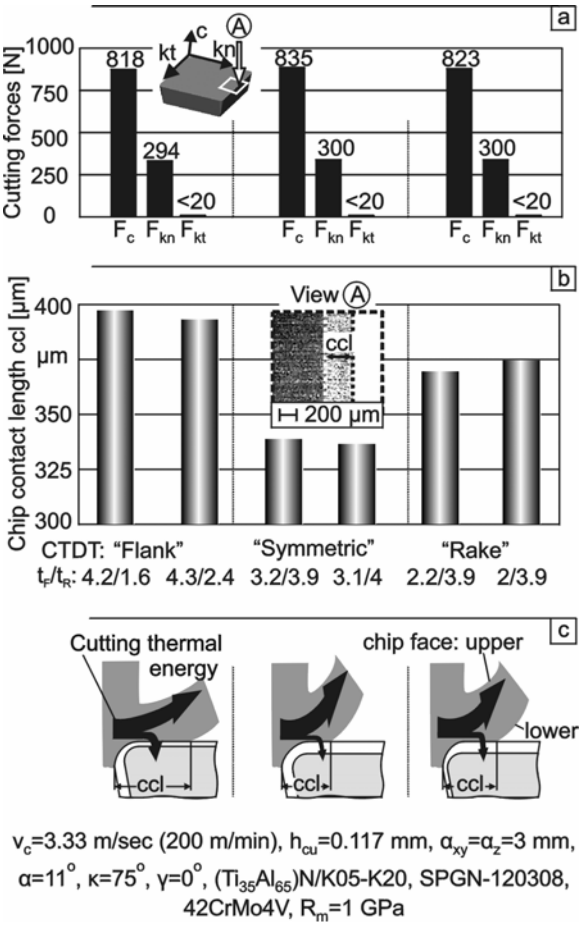

Figure 8: *Measured cutting force components and chip contact lengths ccl, considered in the FEM model of the milling process.*

The "flank" type inserts, demonstrated increased chip contact lengths ccl in comparison to all other cases, whereas the lowest ccl values were detected in milling with "symmetric" inserts.

The thermal energy generated during cutting, is removed mainly by the formed chips. A small part of this energy, as it is indicated in figure 8c, flows into the tool. Herein the coatings act as thermal flux barriers affecting significantly the heat transfer into the tool. In the case of the “symmetric” type inserts the comparatively smallest amount of the total cutting thermal energy is transferred into the tool.

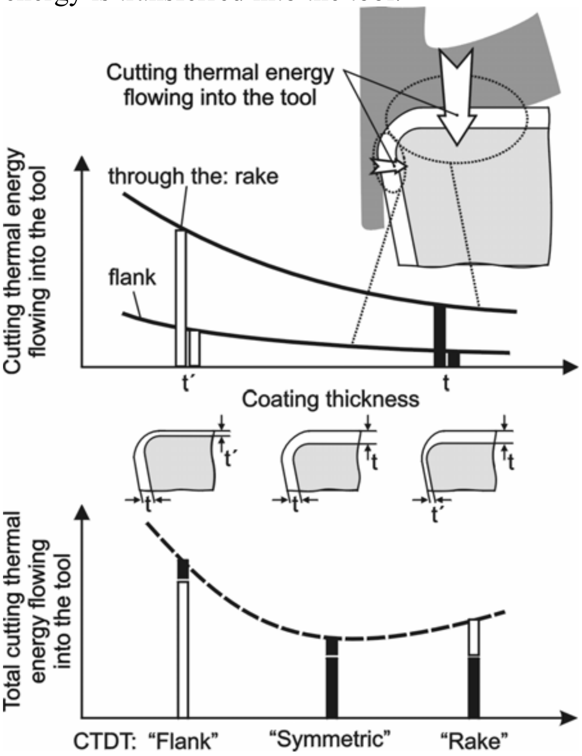

Figure 9: *Cutting thermal energy flowing into the tool through the rake and flank.*

This mechanism takes place due to the increased coating thickness on rake and flank, leading to a higher temperature gradient between the upper and lower chip faces and hence to an intense chip bending and a simultaneous decreasing of the chip contact length ccl. Taking this flowing chip bending mechanism into account and according to the measured ccl values on the various insert types, the chip is less bent in the “rake” type insert and even more less in the “flank” type one in comparison to the “symmetric” cutting plate cases.

These dependencies can be explained considering the cutting thermal energy amounts flowing into the tool through the rake and flank, as it is qualitatively illustrated in the upper part of figure 9. The major part of the cutting thermal energy transferred into the tool, flows through the rake whereas a wide contact between the removed material and the tool exists and the rest energy part through the tool flank [14]. This heat transfer into the tool diminishes by a coating thickness increasing. As it can be observed in the bottom figure part, in the case of the “flank” type inserts, mainly due to the reduction of coating thickness on the rake, the largest amount of the total cutting thermal energy is transferred into the cutting insert in comparison to all other cases. On the other hand the amount of total cutting thermal energy flowing into the tool is minimized in the symmetric insert cases.

Applying the FEM models presented in figure 7, considering the previously described results, the stress distributions in the coating during the material removal can be calculated and the wear behaviour with various coating thicknesses and mechanical strength properties can be explained. The stress distributions during milling, in three characteristic coating thickness distribution cases, are shown in figure 10. In the case of a “flank” type insert, the maximum developed stress of 2.95 GPa, over a wide region in the transient cutting wedge area between flank and rake is above the coating yield strength, which amounts to only 2.8 GPa (see figure 10a). The corresponding overall superficial length OSL of the overstressed area is approximately 5.8 μm. Due to the deteriorated coating mechanical strength, mainly on the flank as indicated in the figure, the overstressed region is damaged, thus leading to a coating failure on the flank after a low number of cuts and to an intensive further wear development. The corresponding stress distribution in the “rake” type insert case is shown in figure 10b. On the flank, the maximum occurring stress is again 2.95 Gpa, however the overstressed area becomes smaller (OSL≈ 0.6 μm) in comparison to the “flank” type insert due to the mechanical strength properties distribution, as shown in figure 10b. Consequently the wear behaviour is improved. The stresses in the “symmetric” insert type are slightly lower in comparison to the corresponding ones in both previously described cases and smaller than the coating yield strength as illustrated in figure 10c. Hence the coating fatigue failure risk is reduced and the wear behaviour is improved.

Figure 11a gives an overview of the observed wear behaviour in all investigated insert type cases. The number of cuts up to various flank wear widths versus the applied insert types are demonstrated. The decreasing of the coating thickness on the flank in the case of a “rake” type insert leads to a worse wear behaviour.

.

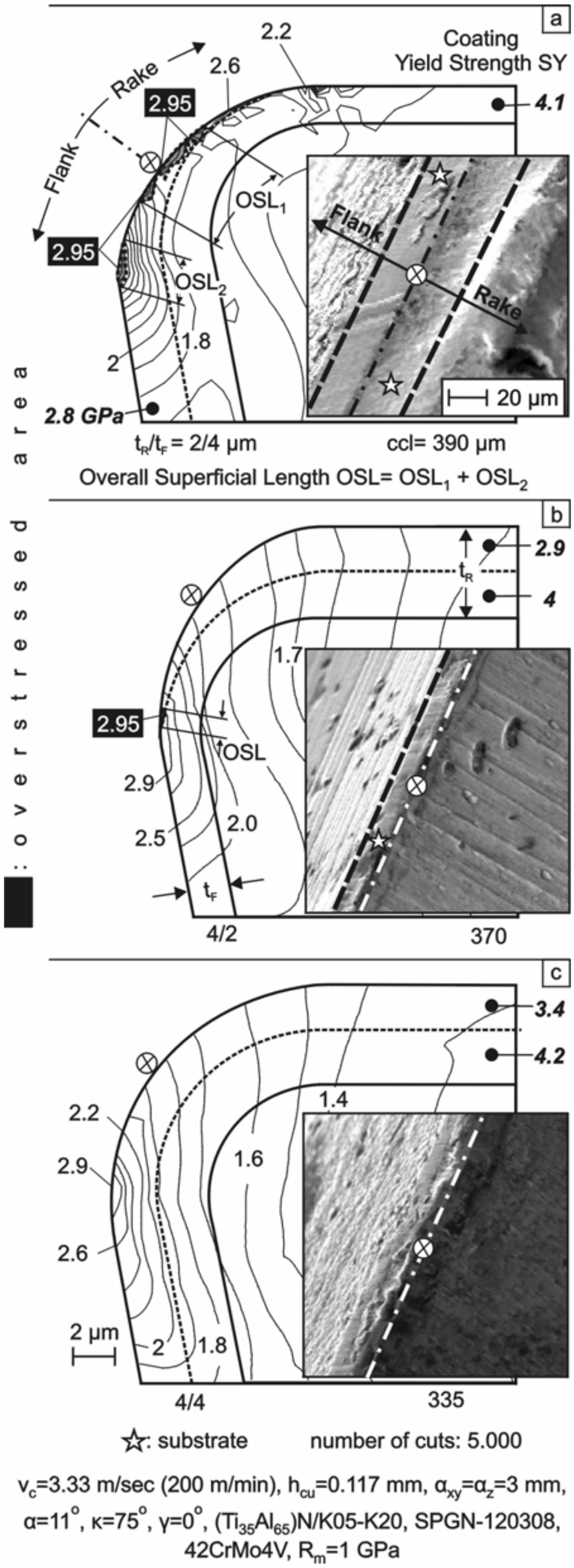

Figure 10*: Stress distributions in the cutting edge region during milling in three characteristic coating thickness distribution cases.*

This deterioration is more significant in the case of the "flank" type inserts, if the coating thickness on the rake decreases. For example, a coated specimen with film thicknesses on the flank and on the rake t_F/t_R [μm]= 3.5/1.1≈ 3.2 respectively ("flank" type) cuts only 21.000 times up to a flank wear width of 0.2 mm, while a "rake" type insert with similar but reverse distributed coating thicknesses (t_R/t_F [μm]= 3.9/1.4≈ 2.8) leads to approximately three times higher number of cuts up to the same flank wear. The best cutting performance was obtained in the case of the "symmetric" inserts.

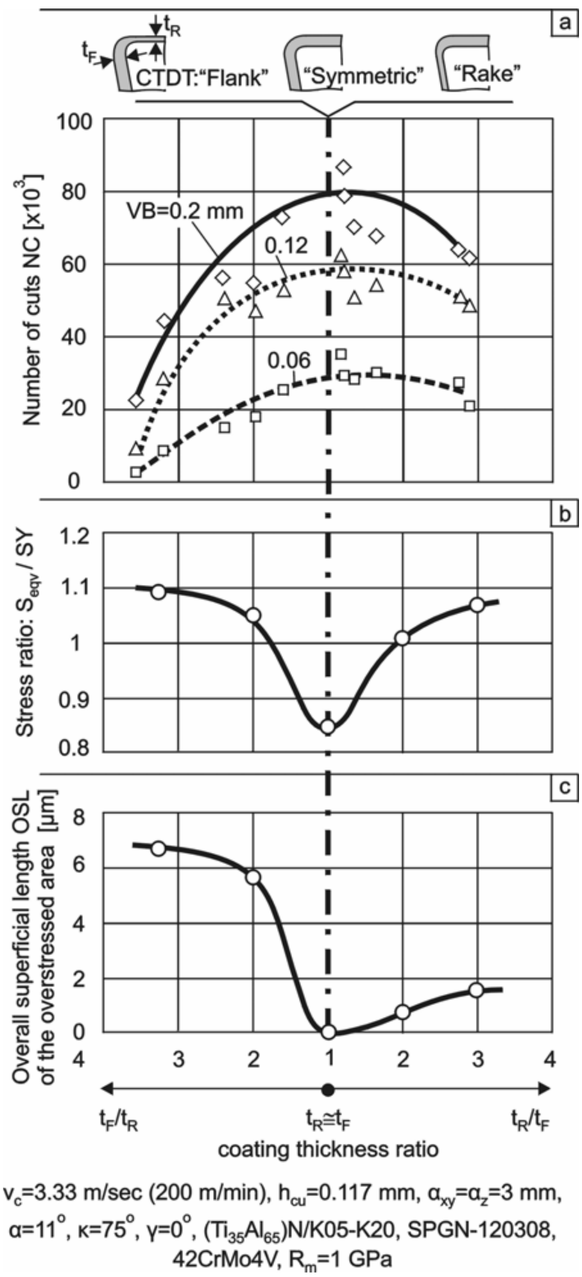

Figure 11: *Wear development and film stress characteristic data in all investigated insert type cases.*

The ratio of the maximum von Mises stresses S_{eqv} in the cutting wedge region to the film yield strength SY are presented in figure 11b. In the "symmetric" coating inserts this ratio is comparatively lower. At approximately equal thickness ratio in the "flank" or "rake" insert types, the related stress ratios are approximately equal. However in the case of the "flank" type inserts, an overstressed area is formed over a significantly larger area on the transient region between flank and rake (see figure 11c), hence contributing to an intensive wear propagation. Moreover despite the similarly high stress ratios, the wear propagation is less intensive in the case of the "rake" type inserts, since the overstressed area is confined in a small superficial cutting wedge region, as demonstrated in figure 11c. The FEM calculated results are in good accordance with the previously described wear results in milling.

5. CONCLUSIONS

PVD TiAlN coated cemented carbide inserts, with variously distributed film thicknesses on the rake and flank have been investigated with regard to their strength properties and milling performance. The mechanical strength properties of the coatings have been determined using a FEM - supported evaluation procedure of nanoindentation measurement results. The extracted experimental and theoretical results indicate that a coating thickness decrease on the tool rake after the film deposition significantly affects the milling performance in comparison to a corresponding decrease on the tool flank. A quasi symmetric distribution of the coating thickness on tool rake and flank leads to an enhanced cutting performance.

6. REFERENCES

[1] Rointan.F. Bunshah, Handbook of Hard Coatings, Noyes Publications / William Andrew Puplishing, LLC, Norwich, New York, U.S.A, (2001).

[2] F. Klocke, T. Krieg, Coated Tools for Metal Cutting – Features and Applications, Annals of the CIRP, 42/2 (1999) 515-525.

[3] K.-D. Bouzakis, N. Michailidis, S. Hadjiyiannis, K. Efstathiou, E. Pavlidou, G. Erkens, S. Rambadt, I. Wirth, Surface and Coatings Technology, vol. 146-147 (2001) 443-450.

[4] H.K. Tönshoff, B. Denkena, T. Friemuth, C. Spengler, Influence of different grinding processes on coating adhesion on cutting tools, Proceedings of the 3rd International Conference "The" Coatings in Manufacturing, (2002) 3-16.

[5] K.-D., Bouzakis, N. Michailidis, G. Skordaris, S. Kombogiannis, S. Hadjiyiannis, K. Efstathiou, E. Pavlidou, G. Erkens, S. Rambadt, I. Wirth, Surface and Coatings Technology, vol.163-164 (2003) 625-630.

[6] K.-D. Bouzakis, S. Hadjiyiannis, G. Skordaris, I. Mirisidis, N. Michailidis, K. Efstathiou, E. Pavlidou, G. Erkens, R. Cremer, S. Rambadt, I. Wirth, Surface and Coatings Technology 177-178 (2004) 657-664.

[7] K.-D. Bouzakis, S. Hadjiyiannis, G. Skordaris, J. Anastopoulos, I. Mirisidis, N. Michailidis, K. Efstathiou, O. Knotek, G. Erkens, R. Cremer, S. Rambadt, I. Wirth, Surface and Coatings Technology, 174-175 (2003) 393-401.

[8] R. Messier, A. P. Giri, R. A. Roy, J. Vac. Sci. Technol. A, 2:500 (1984).

[9] R. Messier, J. Vac. Sci. Technol. A, 4:490 (1986).

[10] R. Messier, J. E. Yehoda, J. Appl. Phys., 58:3739 (1985).

[11] K.–D. Bouzakis, N. Michailidis, S. Hadjiyiannis, G. Skordaris, G. Erkens, Material Characterization, vol. 49-2 (2003) 149-156.

[12] K.–D. Bouzakis, N. Michailidis, S. Hadjiyiannis, G. Skordaris, G. Erkens, Zeitschrift für Metallkunde, 93 (2002) 862-869.

[13] SWANSON Analysis System, INC., ANSYS user manuals, Vol.1 Theory, Vol.2 Procedures, Vol.3 Elements, Vol.4 Commands, (1995).

[14] W. Koenig, F. Klocke,Fertiqungsve-rfahren 1. Drehen, Fraesen, Bohren, 7th improved edition (2002) ISBN 3-540-43304-X, Springer-Verlag Berlin Heidelberg.